

Surface Rolled-in Defects of Titanium Hot Roll Band in HSM

WEI-LIN WANG*, MING-TAO WU*, CHAO-CHI HUANG*,
YEONG-TSUEN PAN** and SZU-NING LIN*

*Iron & Steel Research & Development Department
**New Materials Research & Development Department
China Steel Corporation

The oxide scale produced in the steel making process should be considered due to its after effect on surface quality. For manufacturing Commercially Pure Titanium (CP Ti) hot roll band, the HSM should tune many of the process parameters to adapt for the physical properties of titanium. In this study, the occurrence of top and bottom surface defects related to the oxidation behavior during the hot rolling process is investigated and analyzed using XRD, SEM and TEM. Based on the mechanism of titanium oxidation, only rutile TiO_2 can be regarded as the oxide scale. The titanium suboxides (Ti_xO , $x = 2, 3$, and 6) forming underneath the TiO_2 oxide scale belong to a kind of oxygen interstitial solid solution. After analyzing the microstructure of the titanium matrix, oxide layer and defect/matrix interface, we found that the titanium surface is easily scratched at high temperatures by the HSM equipment such as the side guide, pinch roll and baffle board. These scratched titanium slices will oxidize further and then be rolled into the surface easily. By scrutinizing the crystalline phase and chemical composition of rolled-in defects, the formation mechanism of defects can be established.

Keywords: Commercially Pure Titanium (CP Ti), Surface quality, Oxide scale, Rolled-in defect

1. INTRODUCTION

Titanium and its alloys have been used in various field applications over the past few decades due to their outstanding mechanical and corrosion-resistant properties⁽¹⁻³⁾. Besides mechanical properties, the surface quality is also essential in some applications, especially as decorative parts⁽²⁾. Modification of the surface quality can be conducted during the hot rolling process associated with titanium's physical properties, e.g., oxidation and deformation behavior. Commercially Pure Titanium (CP Ti) is a special reactive and electropositive metal material. It can form adherent, diffusion-resistant oxide layers that protect Ti from both aqueous corrosion and high-temperature oxidation⁽¹⁾.

The CP Ti crystallizes in a modified ideally hexagonal close-packed (hcp) structure at a low temperature, is called α -Titanium (α -Ti), as shown in Fig.1(a). At a high temperature, the body-centered cubic (bcc) structure referred to as β -Ti is stable. The α - β transition temperature of pure Ti is $882 \pm 2^\circ\text{C}$ ⁽²⁾. A slight increase in volume occurs macroscopically during cooling through the β -to- α transformation temperature, which may lead to the large displacements in some directions for a large-sized Ti slab during hot rolling. Some defects may then be induced due to the contact between the Ti slab and the roller assemblies.

On the other hand, the plastic deformation of β -Ti is easier than that of α -Ti because of the number of slip systems (the number of slip systems for the bcc structure is 12 while it is only 3 for the hcp structure)^(2,3). The rolling parameters should be adjusted to meet the requirements for the metal with a specific crystal structure. Moreover, the oxidation behavior must also be taken into account because of the high solid solubility of oxygen in Ti (up to about 33 at.%)⁽⁴⁾ and the variety of the titanium oxides, which may highly influence the descaling effects.

In the present study, typical surface defects on the top and bottom sides of the finish hot-rolled Ti sheet were analyzed and discussed. The frequency of occurrence and formation of various surface defects changes as the rolling parameters were adjusted. By analyzing the defect microstructures, oxidation behavior, and comparing the rolling parameter adjustments, a possible mechanism of the defect formation is suggested.

2. EXPERIMENTAL PROCEDURE

The crystal structure of the surface defects of hot-rolled Ti plate was identified via X-ray diffractometry (D8 Advance, Bruker AXS). Samples of top and cross-sectional surfaces were characterized using a scanning electron microscope (6300, JEOLTM, Japan) equipped with EDS operated at 15 kV. The cross-

sectional TEM specimens were prepared using a Focused Ion Beam (FIB) method. The cross-sectional microstructures were then analyzed using a field-emission Transmission Electron Microscope (TEM, Tecnai G2 F20, FEI, Hillsboro, OR) equipped with EDS. The accelerating voltage was 200 kV.

3. RESULTS AND DISCUSSION

3.1 The nature of CP Ti and oxide scales formed in HSM

Titanium can be alloyed with oxygen due to the solubility of oxygen in α -Ti is essentially larger than in other metals⁽⁵⁾. Because the Ti-O bond energy of 2.2 eV is lower than the Ti-Ti bond energy of 2.56 eV⁽⁶⁾, titanium has an excellent chemical affinity to oxygen. The oxygen atoms dissolved in the α -Ti will occupy the octahedral interstitial sites of the host hcp lattice and these interstitial sites are surrounded by six Ti atoms^(7,8). Figure 1(a) shows the hcp unit cell of α -Ti and the octahedral interstitial sites (\square) for oxygen. The octahedral sites in the hcp lattice form a simple hexagonal lattice with $a = a_{\text{hcp}}$ and $c = c_{\text{hcp}}/2$ where a_{hcp} and c_{hcp} are the lattice parameters of Ti hcp metal lattice.

Corrosion resistance of the CP Ti is contributed by a passive thin layer of titanium oxide which is easily formed at room temperature. Titanium has TiO_2 and three suboxides (Ti_xO , $x = 2, 3$ or 6) in the Ti-O system. No doubt the TiO_2 has been extensively studied and used up to now owing to its unique functional properties. The oxidation of Ti at a high temperature involves the Ti-O interstitial solid solution in the wide range and transformations in them associated with ordering of the structure. These transformations lead to the formation of the suboxides (Ti_xO) of titanium in Ti-O system^(5,9).

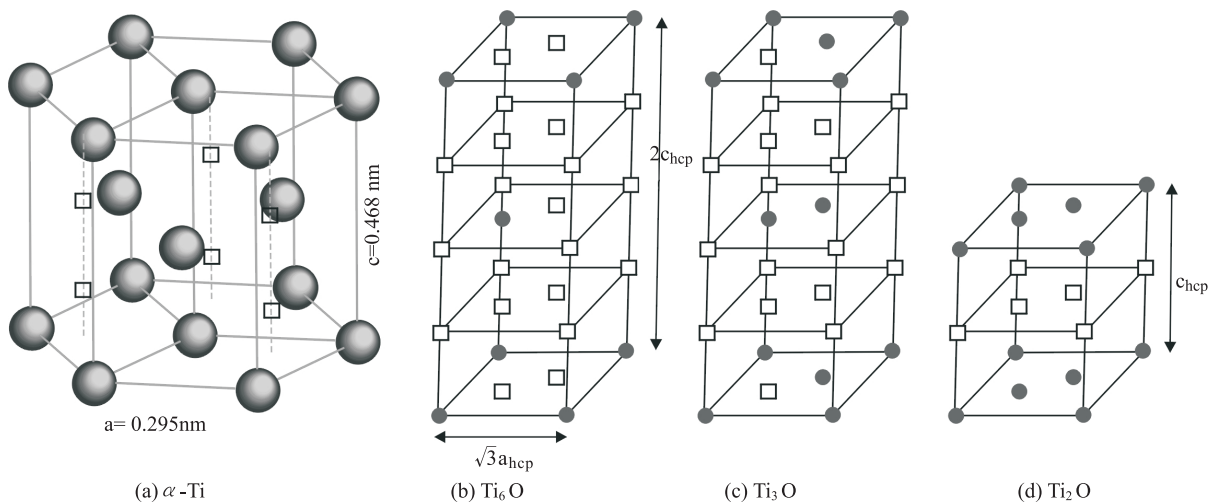


Fig.1. (a) The hcp unit cell of α -Ti and the octahedral sites (\square) for oxygen, (b)-(d) Ti_6O , Ti_3O and Ti_2O oxygen ordered structure, respectively⁽⁸⁾ (where only interstitial sites are shown and filled circles are O atom in the interstitial positions).

The incorporation of O atoms in α -Ti results in a somewhat peculiar variation of the lattice parameters with oxygen content⁽⁷⁾. Figures 1(b)-(d) show the three oxygen ordered structures and all the titanium suboxides Ti_6O , Ti_3O , and Ti_2O have the hcp lattice with an ordered structure. The ordered structures can be viewed as a stacking of interstice layers normal to the c-axis on which oxygen atoms are distributed. The oxygen ordering occurs at and near by the stoichiometric composition of $\text{O/Ti} = 1/3$ ⁽⁷⁾. This phenomenon of oxygen ordering is known to have strong influences on several properties such as hardness, electrical resistivity and thermoelectromotive force^(6,7).

Figure 2 shows TEM micrographs of the oxide scale microstructure of a hot-rolled Ti sheet.

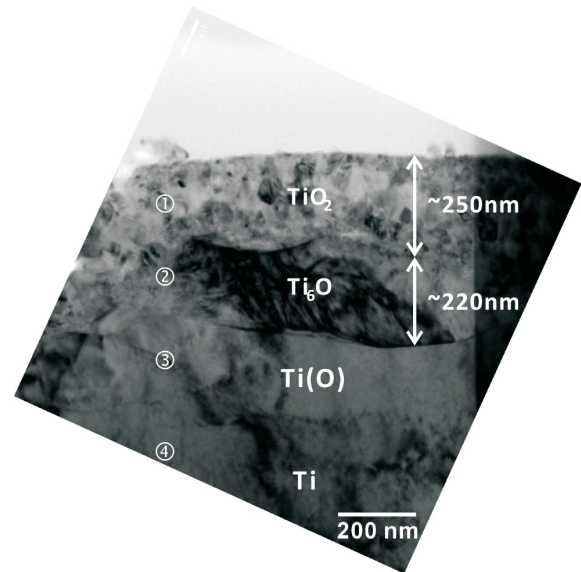


Fig.2. The oxide layer structure of as finished-rolled CP Ti sheets.

The finished-rolled Ti sheet had three oxide layers. The outer layer consisted mainly of stable TiO_2 polycrystalline phase and the intermediate layer consists of a Ti_6O structure. The inner layer belongs to a Ti-O interstitial solid solution (denoted by $\text{Ti}(\text{O})$). The concentration gradient of oxygen was gradually decreased with the distance from the outer layer, indicating the latter two layers were really formed by the diffusion of oxygen in the α -Ti crystal lattice. The total thickness of the oxide layers, only including the outer TiO_2 and intermediate Ti_6O layers, was about $0.5 \mu\text{m}$, which is relatively thin as compared with carbon steels. This is because the TiO_2 formed in the air during the hot rolling process is very protective that the further oxidation of Ti can be prevented. In addition, the rolling force had made the grains of the outer TiO_2 smaller and more compact, unlike the spontaneously formed TiO_2 passive film (less than 10 nm)⁽¹⁰⁾.

3.2 Top surface defects (A33)

Figure 3 shows a representative photograph of rolled-in defects (labeled as A33 defect) which was large in area ($\sim 30 \times 100 \text{ mm}^2$) and found on the top surface of the finished-rolled Ti sheet. Figure 4 shows XRD pattern of the A33 defect, indicating that major TiO_2 and minor Ti_6O co-existed in the A33. The weight ratio of $\text{TiO}_2/\text{Ti}_6\text{O}$ calculated by DQUANT was about 1.77, indicating that higher TiO_2 content near the top surface of A33. Therefore, the A33 defect was supposed to oxidize in the high temperature region for a

certain period of time. The underlying Ti substrate was not detected by XRD because the A33 defect was thicker than $10 \mu\text{m}$. Figure 5 shows top-view secondary electron images (SEI) of the A33 defect and chemical composition analysis obtained from an EDS. Besides Ti and O, an iron (Fe) element about several at.%, was detected in both regions, e.g., spot 1 and 2. The Fe contamination could be attributed to the residual iron oxide from the roller surface or the diffusion of Fe from the roller to the Ti sheet under a high temperature. The Ti/O ratio exceeded 2 even in the low Fe content region (spot 2), indicating that the top surfaces are mainly composed of TiO_2 and titanium suboxide.

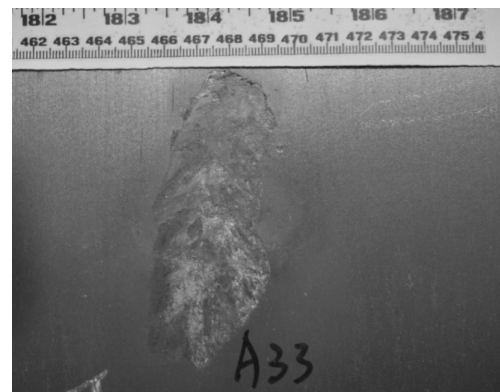


Fig.3. A photograph of the A33 top surface defect.

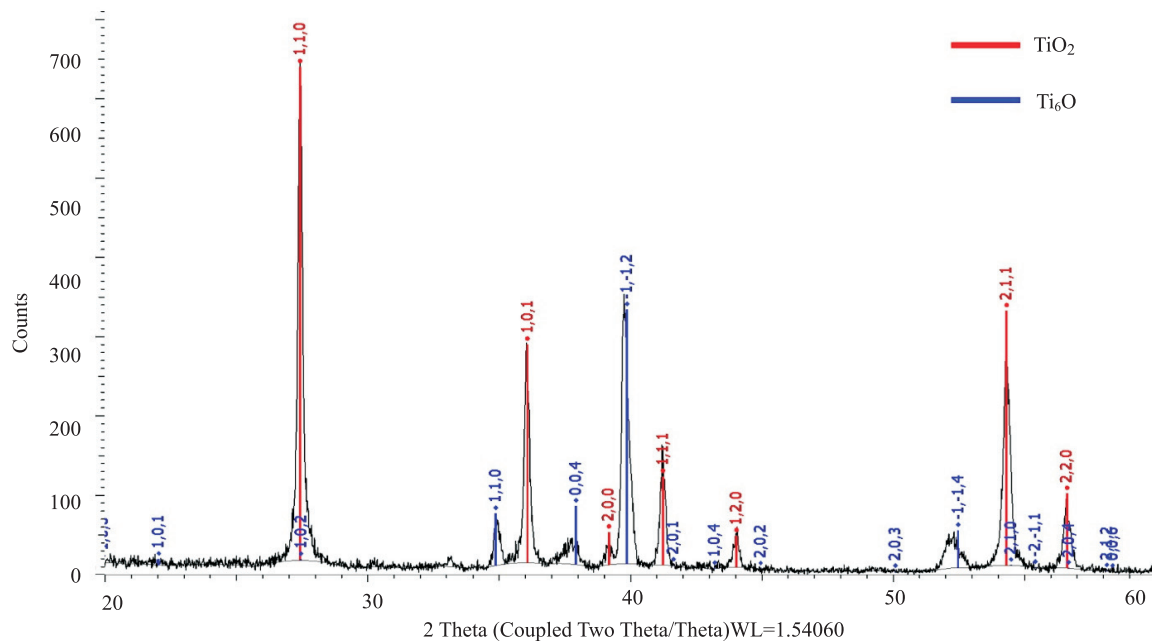


Fig.4. XRD pattern of the A33 top surface.

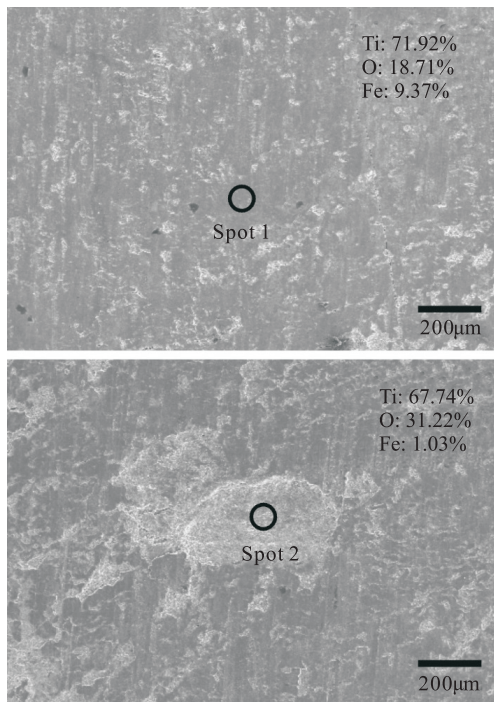


Fig.5. SEM images and chemical composition of the A33 surface.

Figure 6 shows a cross-sectional view of the A33 (only a half part in length is shown). Note that the maximum depth of A33 into the Ti substrate exceeded 1 mm and most regions of the A33 defect have the same image contrast compared with the underlying Ti substrate. Also, the EDS chemical analysis data show the inside of the A33 defect was almost pure Ti. In addition, an important microstructural feature was found inside of the A33. There were some cracks appearing in the A33 and near the A33/Ti substrate interface, which means the A33 defect was not a whole integral piece, but an aggregation of several pieces. A high magnification image and EDS analysis at the A33/Ti interface is shown in Fig.7. The Ti/O ratio of all the dark contrast regions was almost lower than 0.5, whereas no oxygen was detected in the bright contrast regions (spot 1, 5 and 6). Therefore, the phases of dark and bright regions were considered as titanium oxide (mainly TiO₂) and pure Ti, respectively. Also note that the arrangement of material forming sequence from the bottom of A33 to the underlying Ti are Ti/TiO₂/interface/TiO₂/Ti, which suggests that the A33 defect could

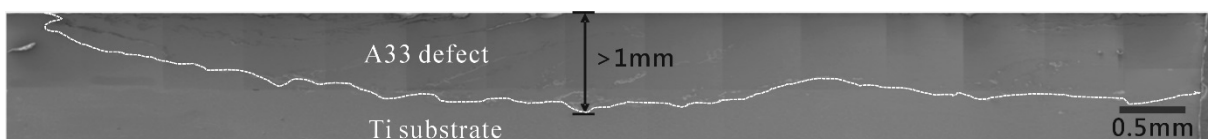
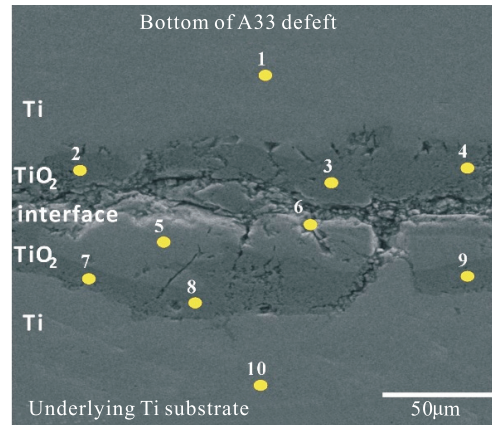


Fig.6. Cross-sectional view of the A33 (only a half of this defect in length is shown).

be an external Ti scrap and then unintentionally fell onto the Ti sheet during the rolling process. Owing to the thick thickness of titanium oxide scale (> 10 µm), the Ti scraps should have been oxidized for a while and covered by fully oxidized thick TiO₂ oxide. Then, they fell and were accidentally rolled into the top surface of Ti sheet, leading to this kind of oxide scale distribution.



Spot	Contrast	Ti	O	C	Ti/O
1	bright	90.16	—	9.84	—
2	dark	28.66	48.49	22.84	0.59
3	dark	26.55	67.24	6.21	0.39
4	dark	28.11	63.80	8.10	0.44
5	bright	100	—	—	—
6	bright	89.43	—	10.57	—
7	dark	23.53	68.69	7.78	0.34
8	dark	23.83	70.45	5.71	0.34
9	dark	27.32	68.12	4.56	0.40
10	bright	64.95	26.83	8.22	—

Fig.7. Chemical composition analysis of the interface nearby the bottom of A33 and underlying Ti substrate.

3.3 Bottom surface defects (A34)

Figure 8 shows a representative image of rolled-in surface defects often found on the bottom side of finished-rolled Ti sheets (labeled as A34). The characteristics of A34 defect were small (usually < 5 mm) and distributed along two edge sides of the Ti sheet. In order to figure out the cause of the A34 surface defect, we investigated and analyzed two cross-sectional regions of the defect, as schematically shown in Fig.8(c). The first one was the top region (i.e. the outer surface) and the second one was the region opposite to the bottom of

A34 defect (i.e. the region located beneath A34 defect). Both the regions were sampled via a FIB technique and analyzed by TEM and EDS. Figure 9(a) shows the ion beam micrograph of a thin slice cut from the A34 top surface and 9(b) shows the corresponding TEM-BF image. Figures 9(c) and 9(d) show the EDS analysis for the outer layer and intermediate layer, respectively. The chemical composition analysis shows the outer layer was TiO_2 oxide (Ti: 37.2%, O: 62.1%, Cr: 0.6% and Fe: 0.1%, in at.%) and the intermediate layer was regarded as an oxygen diffusion zone⁽²⁾ in Ti (Ti: 77.3%, O: 22.6%), denoted as Ti(O).

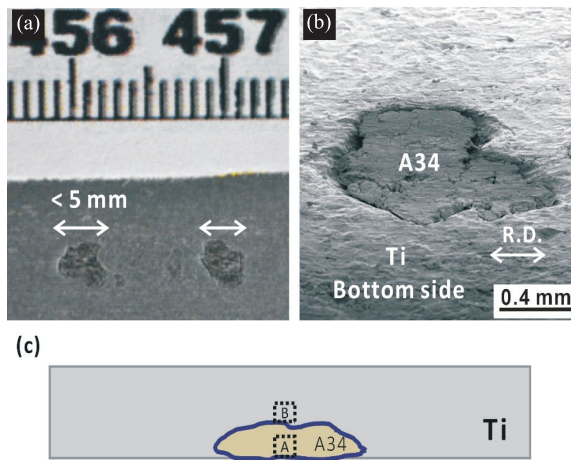


Fig.8. (a) Photograph of the A34 bottom surface defect, (b) SEM image, showing the A34 was rolled onto the Ti surface, (c) Schematic diagram showing the analyzed regions (note the defect is exaggerated for easy identification).

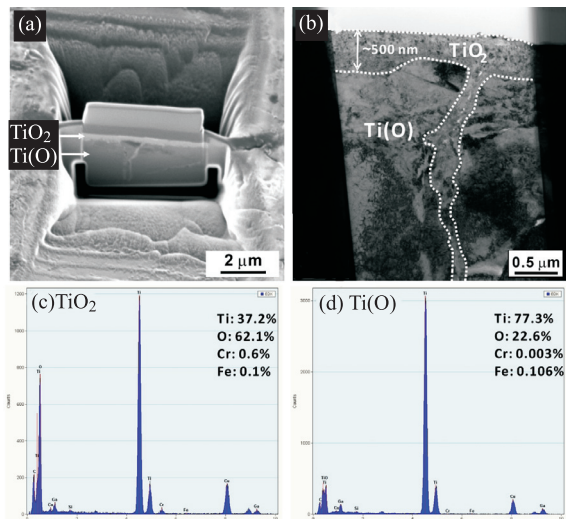


Fig.9. (a) Cross-sectional view of the A34, (b) TEM micrograph of the A34, (c)-(d) EDS chemical analysis of the TiO_2 and Ti(O) regions, respectively.

Therefore, the appearance of oxide scale structure in the A34 was TiO_2 outer layer, Ti(O) intermediate layer and innermost pure Ti. Owing to the material forming sequence of $\text{TiO}_2/\text{Ti(O)}/\text{Ti}$, the A34 defect is considered as rolled-in Ti scraps. Note the outer TiO_2 layer that minor Cr and Fe contents were alloyed with the outer surface of the rolled-in Ti scraps. So, it reasonably suggests that the origin of Ti scraps may come from pure Ti slabs being scratched by the table rollers. After that, attached pure Ti scraps on the table rollers continues to oxidize and react with the roller (Fe-Cr alloy) and then rolled onto the bottom-side of the Ti surface during the rolling process.

In order to find out when the A34 defect was rolled onto the Ti surface, the A34 defect was removed from the Ti sheet and the top surface and cross-sectional regions underneath the A34 defect were analyzed, as shown in dashed rectangle B in Fig.8(c). Figure 10(a) shows the top surface morphology underneath the A34 defect and 10(b) shows a thin sliced specimen cut from a center position of Fig.10(a). In Figure 10(b), the microstructure consisted of three layers ($\text{TiO}_2/\text{Ti(O)}/\text{Ti}$), similar to the A34 top surface oxide structure. Compared with the Fig.9(a), the TiO_2 oxide layer ($\sim 150 \text{ nm}$) was thinner than the top surface of A34 ($\sim 500 \text{ nm}$), implying that the oxidation reaction was inhibited. It is reasonable because the supply of oxygen gas beneath the Ti scraps was much less than the outermost surface of the A34 defect. Figures 10(c) and 10(d) show TEM bright-field images of the specimen in 10(b). In Figure 10(d),

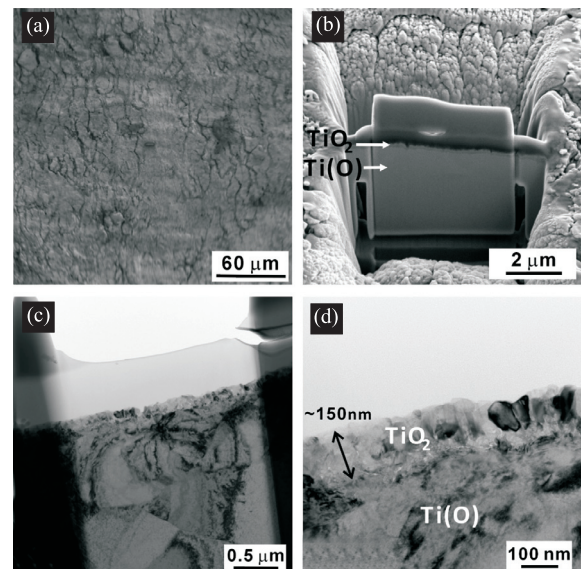


Fig.10. (a) Top surface morphology underneath the A34 defect (b) SEM image showing the FIB thin slice specimen cut from (a), (c)-(d) TEM micrographs of the specimen.

we observed that the surface layer TiO_2 grains underneath the A34 exhibited larger average grain size (~ 100 nm), which is very different from that fine and small TiO_2 grains occurred in the outer A34 surface layer (shown in Fig.9(b)). It therefore suggests that the A34 surface defect should be an attached-in or rolled-in defect. Considering the relationships of defect characteristics, the hot rolling process and oxidation behavior at high temperature, we propose that the A34 defect belongs to rolled-in Ti scraps which were brought onto the Ti sheet after the Scale Breaker (SB) process.

4. CONCLUSIONS

Titanium is a lightweight metal having good corrosion resistance, good mechanical properties and is beginning to have more and more applications in outdoor exposed environments. For manufacturing CP Ti hot rolled band in HSM, the surface quality is needed to be highly controlled and continuously improved. In this study, the typical top and bottom rolled-in surface defects appearing in the finished-rolled Ti sheets are investigated. The following conclusions were drawn from our analysis:

1. The oxide layer structure of as-rolled Ti sheet is mainly composed of three layers: outermost TiO_2 , intermediate Ti_6O and innermost Ti-O oxygen solid solution. The total thickness of the former two phases is about $0.5 \mu\text{m}$, which is relatively thin as compared with carbon steel.
2. The top surface defect is regarded as external and large Ti scraps which fall unintentionally and rolled into the Ti surface during hot rolling.

3. The bottom surface defect is considered as rolled-in or attached-in Ti scraps which come from pure Ti slabs scratching against the table rollers.

REFERENCES

1. A. M. Russell and K. L. Lee: Structure-property Relations in Nonferrous Metals, J. Wiley & Sons, New Jersey, 2005, pp. 179-197.
2. C. Leyens and M. Peters: Titanium and Titanium Alloys. Fundamentals and Applications, Wiley-VCH, Weinheim, 2003.
3. J. C. M. Li: Microstructure and Properties of Materials. World Scientific Publishing, 2000, Singapore, pp. 1-77.
4. J. L. Murry and H. A. Wriedt: J. Phase Equil., 1987, vol. 8, pp. 148-165.
5. I. I. Kornilov: Metal Science Heat Treatment., 1973, vol. 15, pp. 826-829.
6. H. Ma, M. Wang and W. Wu: J. Mater. Sci. Technol., 2004, vol. 20, pp. 719-723.
7. S. Banerjee and P. Mukhopadhyay: Phase Transformations. Examples from Titanium and Zirconium Alloys, Pergamon, Amsterdam, 2007, pp. 764-784.
8. A. V. Ruban, V. I. Baykov and B. Johansson: Phys. Rev. B, 2010, vol. 82, pp. 134110-1--134110-10.
9. B. Holmberg: Acta Chemica Scandinavica, 1962, vol. 16, pp. 1245-1250.
10. E. Gemelli and N. H. A. Camargo: Revista Materia, 2007, vol. 12, pp. 525-531. □